

Synthesis, Characterization and Photophysical Properties of ESIPT Reactive Triazine Derivatives

*Marcelo D. Kuplich, Fábio S. Grasel, Leandra F. Campo,
Fabiano S. Rodembusch and Valter Stefani**

*Laboratório de Novos Materiais Orgânicos, Instituto de Química, Universidade Federal do
Rio Grande do Sul, Av. Bento Gonçalves 9500, CP 15003, 91501-970 Porto Alegre-RS, Brazil*

Uma série de quatro compostos fotoativos derivados da triazina foi obtida a partir da substituição nucleofílica aromática no cloreto cianúrico. Os compostos foram caracterizados por espectroscopia de infravermelho (IR) e ressonância magnética nuclear (NMR de ^1H e ^{13}C), além de espectrometria de massas de alta resolução (HRMS MALDI). A espectroscopia de absorção na região do UV-Vis e a emissão de fluorescência (no estado sólido e em solução) foram também utilizadas para estudar o comportamento fotofísico destes compostos. Os derivados obtidos são fluorescentes na região do azul-laranja por um mecanismo de transferência protônica intramolecular no estado excitado e apresentam um grande deslocamento de Stokes ($6365\text{-}10290\text{ cm}^{-1}$). Os derivados sintetizados neste trabalho reagiram com sucesso com fibras de celulose para dar novos compostos celulósicos fluorescentes.

Four new reactive fluorescent triazine derivatives were obtained from nucleophilic aromatic substitution of cyanuric chloride. The compounds were characterized by infrared spectroscopy (IR), nuclear magnetic resonance (^{13}C and ^1H NMR) and high resolution mass spectrometry (HRMS MALDI). UV-Vis and steady-state fluorescence (in solution and in solid state) spectroscopies were also applied to characterize the photophysical behavior. The dyes are fluorescent by an intramolecular proton transfer mechanism (ESIPT) in the blue-orange region, with a large Stokes shift between $6365\text{-}10290\text{ cm}^{-1}$. The fluorescent cyanuric derivatives could successfully react with cellulose fibers to give new fluorescent cellulosic materials.

Keywords: triazine, benzazoles, cyanuric chloride, ESIPT, reactive dyes, cellulose

Introduction

The 2,4,6-trichloro-1,3,5-triazine (TCT), so-called cyanuric chloride, is an important triazine derivative and a well-known precursor in organic synthesis.¹⁻¹¹ This precursor have become a very attractive field of research by virtue of the applications that can be envisaged with the obtained products, such as polymers,¹²⁻¹⁵ non-linear optical materials¹⁶⁻¹⁸ and new photoactive materials.¹⁹⁻²³ A particular interest has been reported on the use of cyanuric chloride in reactive dyes²⁴ since they are able to bond hydroxy groups from the cellulose and amino or thiol from proteins or polyamides.²⁵ In this way, several structures have been reported using TCT as molecular link between the chromophore or fluorescent dye and the organic matrix.²⁶⁻²⁹

On the other hand, the benzazoles often show a large Stokes shift due to an excited state intramolecular proton

transfer (ESIPT) mechanism.³⁰ This phenomenon has widespread implications as optical sensors,³¹⁻³⁴ photoactive hybrid materials^{35,36} and new polymeric materials.³⁷

Despite of the great attention of ESIPT-exhibiting dyes and the versatile applications of cyanuric chloride in organic synthesis as starting material to produce dyes, herbicides, polymers and compounds of pharmaceutical interest,³⁸ this paper presents the synthesis and the photophysical characterization of new ESIPT reactive dyes based on the triazine moiety. Additionally, the obtained derivatives were tested as fluorophores for cellulosic materials.

Experimental

Materials and methods

2,4,6-Trichloro-1,3,5-triazine were purchased from ACROS Organics. All the solvents were used as received or

*e-mail: vstefani@iq.ufrgs.br

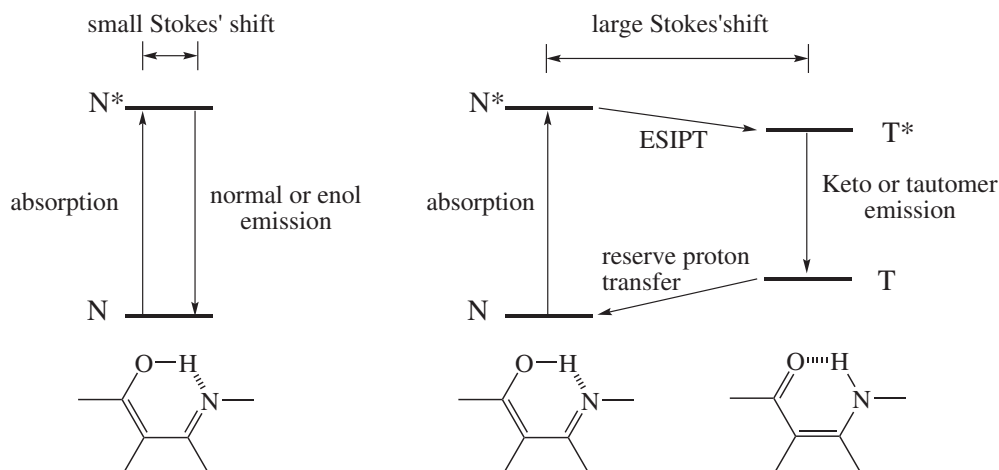


Figure 1. Photophysical pathways from ESIPT-exhibiting dyes: normal (or enol) emission (left) and ESIPT (or tautomer) emission (right).

purified using standard procedures. Spectroscopic grade solvents (Merck) were used for fluorescence and UV-Vis measurements. Melting points (mp) were measured with a Gehaka PF 1000 apparatus and are uncorrected. Infrared spectra were recorded on a Shimadzu FTIR8300 in KBr pellets. ^1H and ^{13}C NMR spectra were performed on a VARIAN INOVA YH300 using tetramethylsilane (TMS) as the internal standard and $\text{DMSO-}d_6$ (Aldrich) as the solvent at room temperature. UV-Vis absorption spectra were performed on a Shimadzu UV-1601PC spectrophotometer. Steady state fluorescence spectra were measured with a Hitachi spectrofluorometer model F-4500. Spectrum correction was performed to enable measuring a true spectrum by eliminating instrumental response such as wavelength characteristics of the monochromator or detector using Rhodamine B as a standard (quantum counter). For the photophysical measurements in the solid state, the photoactive cellulose fibers were measured in bulk using a solid sample holder. In this device, the light beam was irradiated to the sample at an angle of *ca.* 30° , and the light beam from the sample was reflected at an angle of *ca.* -60° . All experiments were performed at room temperature in a concentration of 10^{-6} mol L^{-1} . HRMS spectra were recorded with a Bruker Reflex III spectrometer.

Synthesis of the triazine derivatives

The dyes **1a-d** were prepared using a previously described methodology.³⁹ The triazine benzazole derivatives **3a-d** were prepared according to Figure 2. In a typical experiment, an equimolar amount of the amino derivative **1a-d** and 2,4,6-trichloro-1,3,5-triazine were both dissolved in acetone. The dye solution was added dropwise into the triazine solution, cooled up to 0°C , followed by addition of a Na_2CO_3 solution (10%). The final solution was mixed

for 1 h. The crude product, which precipitates, was washed with water and cold acetone and dried at room temperature. The purification was made by recrystallization using dioxane/water. The final yields were from 70 to 96%.

2-[4'-(*N*-4,6-Dichloro-1,3,5-triazin-2-yl)-2'-hydroxyphenyl] benzoxazole (**3a**)

Yield: 70%; mp $> 350^\circ\text{C}$; IR (KBr) $\nu_{\text{max}}/\text{cm}^{-1}$ 3296 $\nu(\text{N-H})$, 3059 $\nu_{\text{arom}}(\text{C-H})$, 1618 $\nu(\text{C=N})$, 1537 and 1501 $\nu_{\text{arom}}(\text{C=C})$, 1238 $\nu(\text{Ar-O})$, 1188 $\nu(\text{C-N})$, 748 $\nu(\text{C-Cl})$; ^1H NMR (300 MHz, $\text{DMSO-}d_6$) δ/ppm 10.96 (s, 1H, OH), 7.98 (d, 1H, H_6 , J_o 8.7 Hz), 7.88-7.76 (m, 2H, H_4 and H_7), 7.66 (d, 1H, H_3 , J_m 2.0 Hz), 7.50-7.38 (m, 2H, H_5 and H_6), 7.21 (dd, 1H, H_5 , J_m 2.0 Hz and J_o 8.7 Hz); ^{13}C NMR (75.4 MHz, $\text{DMSO-}d_6$) δ/ppm 162 (C_2), 158 (C_{4a}), 154 (C_{4b} and C_{4c}), 153 (C_2), 149 (C_8), 142 (C_4), 139 (C_9), 128 (C_5), 126 (C_6 or C_6), 125 (C_6 or C_6), 119 (C_4), 112 (C_3 or C_7), 111 (C_7 or C_3), 108 (C_5), 106 (C_1); exact mass: 373.0133 g mol^{-1} ; the exact molecular mass for $\text{C}_{16}\text{H}_9\text{Cl}_2\text{N}_5\text{O}_2$ m/z 373.012 was found by HRMS (MALDI).

2-[4'-(*N*-4,6-Dichloro-1,3,5-triazin-2-yl)-2'-hydroxyphenyl] benzothiazole (**3b**)

Yield: 80%; mp $> 350^\circ\text{C}$; IR (KBr) $\nu_{\text{max}}/\text{cm}^{-1}$ 3331 $\nu(\text{N-H})$, 3069 $\nu_{\text{arom}}(\text{C-H})$, 1612 $\nu(\text{C=N})$, 1566 and 1481 $\nu_{\text{arom}}(\text{C=C})$, 1238 $\nu(\text{Ar-O})$, 1186 $\nu(\text{C-N})$, 752 $\nu(\text{C-Cl})$; ^1H NMR (300 MHz, $\text{DMSO-}d_6$) δ/ppm 11.19 (s, 1H, OH), 8.24 (d, 1H, H_3 , J_m 2.7 Hz), 7.94-7.80 (m, 2H, H_4 and H_7), 7.72 (dd, 1H, H_5 , J_m 2.7 Hz and J_o 9.0 Hz), 7.54-7.42 (m, 2H, H_5 and H_6), 7.19 (d, 1H, H_6 , J_o 9.0 Hz); ^{13}C NMR (75.4 MHz, $\text{DMSO-}d_6$) δ/ppm 170 (C_2), 164 (C_{4a}), 162 (C_{4b} and C_{4c}), 155 (C_2), 149 (C_9), 140 (C_4), 129 (C_8),

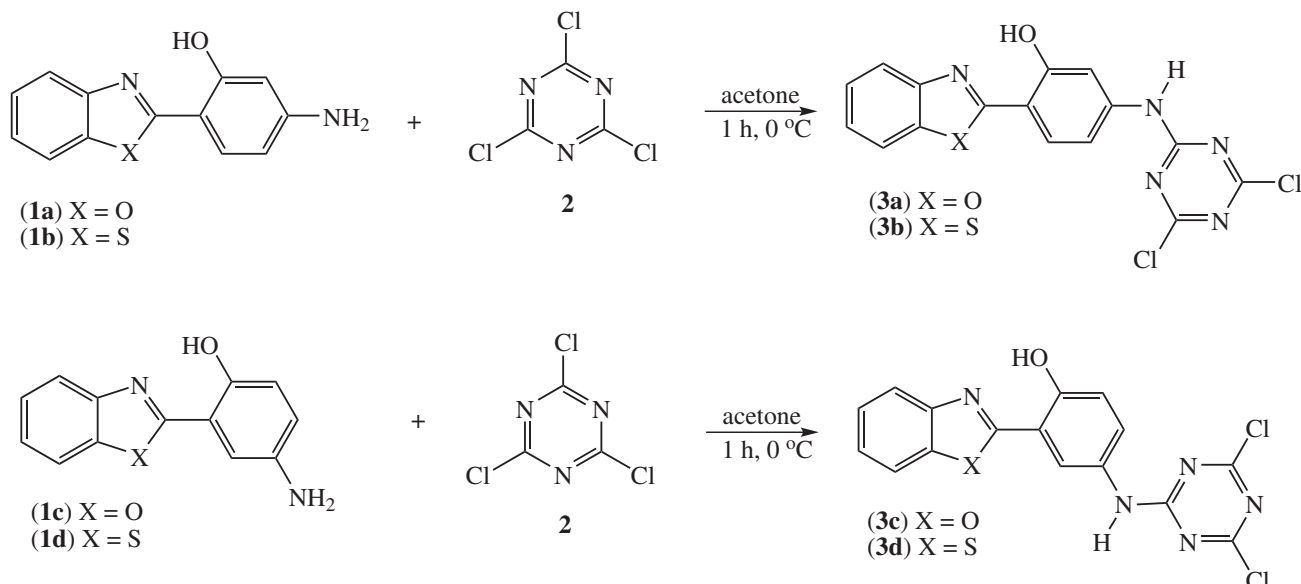


Figure 2. Synthesis of the triazine derivatives **3a-d**.

128 (C₄), 126 (C₅ or C₆), 125 (C₅ or C₆), 121 (C₆), 119 (C₇ or C₃), 118 (C₃ or C₇), 111 (C₅), 110 (C₁); exact mass: 388.9905 g mol⁻¹; the exact molecular mass for C₁₆H₉Cl₂N₅OS *m/z* 388.990 was found by HRMS (MALDI).

2-[5'-(*N*-4,6-Dichloro-1,3,5-triazin-2-yl)-2'-hydroxyphenyl]benzoxazole (**3c**)

Yield: 83%; mp > 350 °C; IR (KBr) ν_{\max} /cm⁻¹ 3302 ν (N-H), 3065 ν_{arom} (C-H), 1616 ν (C=N), 1587 and 1501 ν_{arom} (C=C), 1238 ν (Ar-O), 1167 ν (C-N), 739 ν (C-Cl); ¹H NMR (300 MHz, DMSO-*d*₆) δ /ppm 10.98 (s, 1H, OH), 8.23 (d, 1H, H₆, *J*_m 2.7 Hz), 7.94-7.84 (m, 2H, H₄ and H₇), 7.61 (dd, 1H, H₄, *J*_m 2.7 Hz and *J*_o 9.0 Hz), 7.54-7.44 (m, 2H, H₅ and H₆), 7.17 (d, 1H, H₃, *J*_o 9.0 Hz); ¹³C NMR (75.4 MHz, DMSO-*d*₆) δ /ppm 170 (C₂), 164 (C_{4a}), 162 (C_{4b} and C_{4c}), 155 (C₂), 149 (C₈), 140 (C₉), 129 (C₄), 126 (C₅ or C₆), 125 (C₅ or C₆), 121 (C₄), 119 (C₆ or C₃), 118 (C₃ or C₆), 111 (C₇), 110 (C₁); exact mass: 373.0133 g mol⁻¹; the exact molecular mass for C₁₆H₉Cl₂N₅O₂ *m/z* 373.012 was found by HRMS (MALDI).

2-[5'-(*N*-4,6-Dichloro-1,3,5-triazin-2-yl)-2'-hydroxyphenyl]benzothiazole (**3d**)

Yield: 96%; mp > 350 °C; IR (KBr) ν_{\max} /cm⁻¹ 3285 ν (N-H), 3063 ν_{arom} (C-H), 1556 and 1501 ν_{arom} (C=C), 1238 ν (Ar-O), 1198 ν (C-N), 758 ν (C-Cl); ¹H NMR (300 MHz, DMSO-*d*₆) δ /ppm 11.09 (s, 1H, OH); 8.41 (d, 1H, H₆, *J*_m 2.7 Hz), 8.15 (d, 1H, H₄ or H₇), 8.05 (d, 1H, H₇ or H₄), 7.60 (dd, 1H, H₄, *J*_m 2.7 Hz and *J*_o 9.0 Hz), 7.54 (t, 1H, H₅ or H₆), 7.45 (t, 1H, H₆ or H₅), 7.13 (d, 1H, H₃, *J*_o 9.0 Hz);

¹³C NMR (75.4 MHz, DMSO-*d*₆) δ /ppm 170 (C₂), 169 (C_{5a}), 164 (C_{5b} or C_{5c}), 154 (C₂), 151 (C₉), 135 (C₅), 129 (C₈), 127 (C₅ or C₆), 127 (C₅ or C₆), 125 (C₄), 122 (C₇ or C₄), 122 (C₄ or C₇), 122 (C₆), 118 (C₁), 117 (C₃); exact mass: 388.9905 g mol⁻¹; the exact molecular mass for C₁₆H₉Cl₂N₅OS *m/z* 388.989 was found by HRMS (MALDI).

Dye incorporation into the cellulose fibers

In a typical experiment, the cellulose was stained by addition of the cotton (100 mg) into an aqueous solution of Na₂SO₄ (0.05 mol L⁻¹) and 0.2 ml of sodium hydroxide (10% m/v) followed by the addition of the fluorescent dye (1 mg mL⁻¹ in DMSO). The reaction mixture was allowed to react for 1 h at 45 °C. The crude stained cotton was washed several times with water, followed by Soxhlet extraction using acetone for 3 h in order to remove the unreacted fluorescent dye. The percentages of the triazine dye incorporation were evaluated using the absorption data from UV-Vis spectroscopy. Since the extinction coefficients of the dyes are well-known, the percentages of the triazine dye incorporation, which were from 80 up to 95%, were determined by the reactive dye extinction coefficients at a specific wavelength from UV-Vis data of the washing solutions (Lambert-Beer Law).

Results and Discussion

Photophysical characterization

Figures 3 and 4 show the normalized UV-Vis absorption spectra of the triazine derivatives (**3a-d**) in

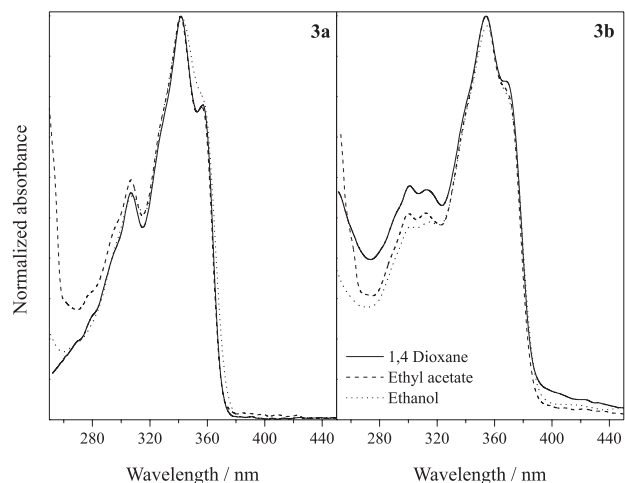


Figure 3. Normalized absorption spectra of **3a-b**.

1,4-dioxane, ethyl acetate and ethanol. The relevant UV-Vis data are summarized in Table 1.

An absorption band maxima (λ_{\max}) located around 358 and 368 nm (with molar extinction coefficient values (ϵ_{\max}) in agreement with π - π^* transitions) could be observed for the derivatives **3a** and **3b**, respectively. A small solvatochromic effect could be observed for these dyes (*ca.* 4 nm). The absorption maximum of **3b** is red shifted in relation to **3a**, which can be explained by the better electron delocalization. This is allowed by the sulfur atom in relation to the oxygen. The same photophysical behavior was observed for derivatives **3c** and **3d**, with an absorption maximum located *ca.* 338 and 352 nm, respectively.

The intense absorption bands observed at 280-310 nm for derivatives **3c-d** indicate that the substitution in the phenolic ring is decisive for the photophysics of these dyes and can be associated to a difference of planarity of the dyes.⁴⁰ A non-planar structure does not allow a

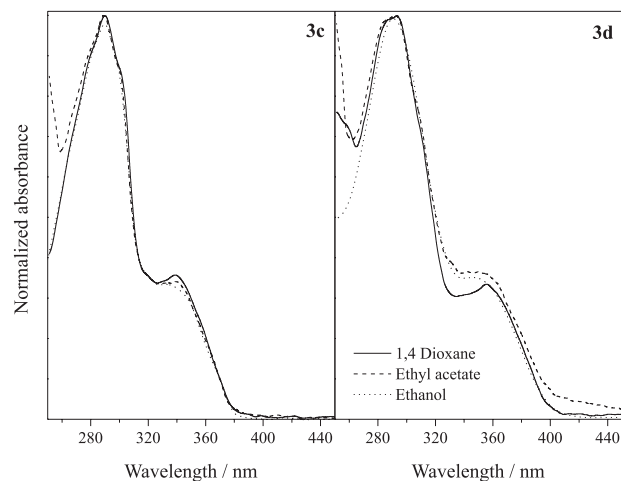


Figure 4. Normalized absorption spectra of **3c-d**.

more effective electronic delocalization among the two π systems (phenolic and benzoxazolic rings). In this way, the *para* derivative showed to be less planar than their *meta* analogue. The intense bands at 280-310 nm are related to the oxazole chromophore.^{41,42} The difference between the molecular planarity of these dyes is confirmed taking the molar extinction coefficient values into account (see Table 1). A less planar structure usually presents a lower probability for the π - π^* transition.

Figures 5 and 6 present the normalized fluorescence emission spectra of these dyes. The curves were obtained using the absorption maxima as the excitation wavelengths. The relevant data are also summarized in Table 1.

The derivatives **3a-d** present one main band located at *ca.* 471, 506, 514 and 546 nm, respectively. In solution, these dyes are fluorescent in the blue-green (**3a-b**) and green-yellow (**3c-d**) regions. The fluorescence emission bands are ascribed to the ESIPT band (T^* emission) since

Table 1. Relevant UV-Vis data of the triazine derivatives **3a-d**

Dye	Solvent	$\lambda_{\text{abs}} / \text{nm}$	$\epsilon_{\text{max}} \times 10^4 / (\text{mol}^{-1} \text{L cm}^{-1})$	$\lambda_{\text{em}} / \text{nm}$	$\Delta\lambda_{\text{ST}} / (\text{nm/cm}^{-1})$
3a	1,4-dioxane	358	4.4	474	116/6836
	ethyl acetate	356	3.1	471	115/6859
	ethanol	360	5.6	467	107/6365
3b	1,4-dioxane	370	5.2	510	140/7419
	ethyl acetate	366	4.4	505	139/7520
	ethanol	367	4.9	504	137/7407
3c	1,4-dioxane	339	1.4	515	176/10081
	ethyl acetate	341	1.4	515	174/9908
	ethanol	335	1.3	513	178/10358
3d	1,4-dioxane	356	1.2	547	191/9809
	ethyl acetate	350	1.9	547	197/10290
	ethanol	350	1.1	544	194/10189

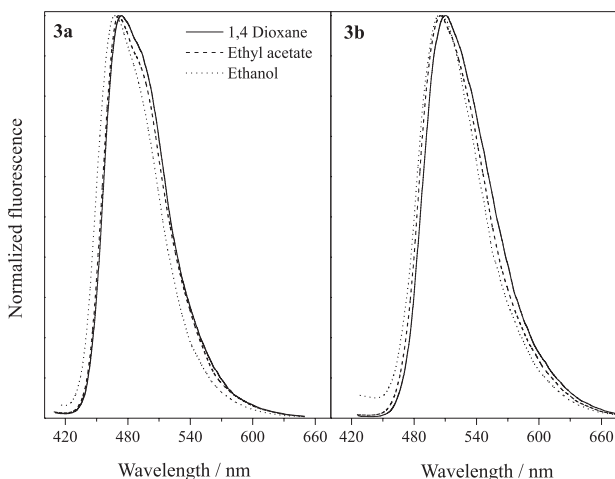


Figure 5. Normalized fluorescence emission spectra of **3a-b**.

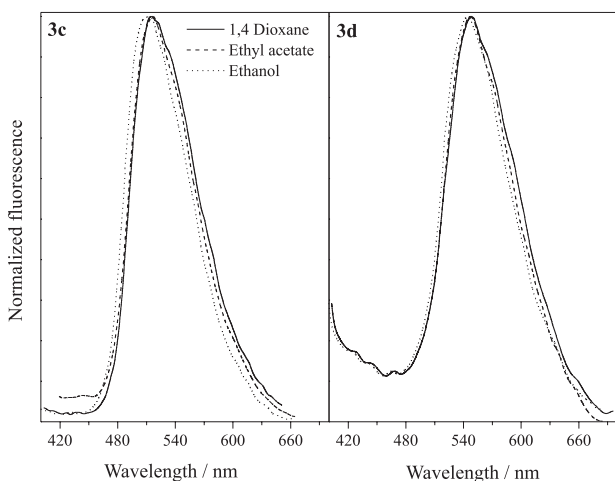


Figure 6. Normalized fluorescence emission spectra of **3c-d**.

a Stokes shift higher than 100 nm could be detected for all dyes.⁴³

Figure 7 shows the normalized fluorescence emission spectra in the solid state of the dyes **3a-d**, as well as the dyes covalently bounded into the cellulose matrix. The absorption maxima in solution were used as excitation wavelength in the solid state measurements. As already observed in solution, the derivatives **3a-d** present one main band located from 459 to 537 nm, which comprises the blue-orange region.

Concerning the location of the fluorescence emission maxima in solution (Table 1), the dyes in the solid state present blue shifted bands (**3a**: 459 nm, **3b**: 508 nm, **3c**: 491 nm and **3d**: 536 nm), indicating that the studied solvents can better stabilize the keto tautomer in the excited state. Additionally, comparing dyes **3a-c** in the solid state and the cellulosic material after the staining process, it can be observed small changes in the fluorescence emission maxima due to the interaction with the cellulose matrix.

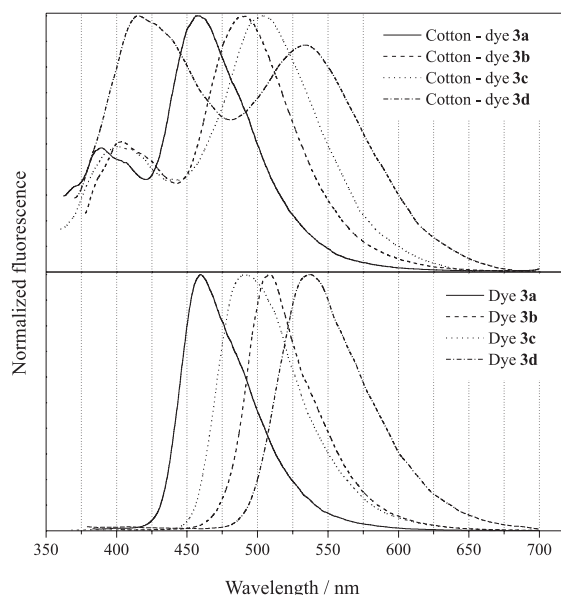


Figure 7. Normalized solid-state fluorescence emission spectra of the derivatives **3a-d** (bottom) and covalently bounded into cellulose fibers (top). This measurement treats the fibers in bulk using a solid sample holder with the light beam irradiated to the sample at an angle of *ca.* 30°, and the light beam from the sample reflected at an angle of *ca.* -60°.

However, after the staining process using dye **3d**, a dual fluorescence emission can be observed in the cellulose. The band located at higher wavelengths is ascribed to the ES IPT band and, the blue shifted one is ascribed to the normal relaxation (N^* emission).⁴⁴ This photophysical behavior confirms a conformational equilibrium in the ground state for this dye. Since the hydroxyl moieties in the cellulose matrix could stabilize through intermolecular hydrogen bond, additional conformers can be related to the normal emission.⁴⁴ A pictorial scheme with the inter (left) and intramolecular (right) hydrogen bonds between the ES IPT dye and the cellulose is presented in Figure 8. Although the synthesized triazine dyes present two reactive chlorine atoms, the reactive dye is shown with only one replaced chlorine atom by the cellulose matrix. This is because the used temperature for the incorporation of the triazine derivatives into the cellulose fibers was below the needed temperature to replace the last chlorine atom.²⁴

Conclusions

Four new fluorescent cotton reactive dyes were synthesized, purified and characterized by infrared spectroscopy, nuclear magnetic resonance (¹³C and ¹H NMR), high resolution mass spectrometry (HRMS MALDI), UV-Vis and steady-state fluorescence spectroscopies (in solution and in the solid state). The triazine derivatives are fluorescent in the blue-orange region with a Stokes shift between 6365-10290 cm^{-1} . The fluorescent cyanuric derivatives could

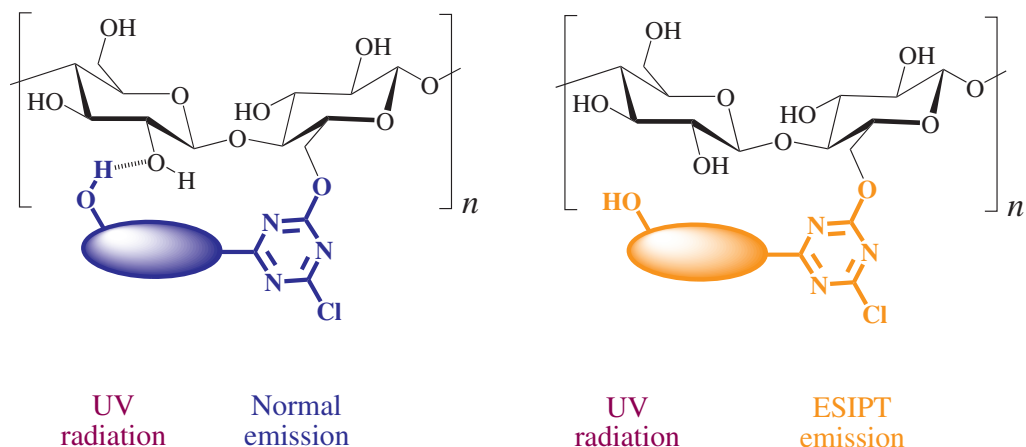


Figure 8. Scheme of interaction between the ESIPT dyes and the cellulose.

successfully react with cellulose fibers to produce new ESIPT fluorescent cellulosic materials. A dual fluorescence emission could be observed in the stained cotton using the dye **3d**, which indicates a conformational equilibrium in solution in the ground state. The emission at long wavelength (ESIPT band) is related to the ESIPT band and, the blue shifted ones are due to conformational forms with a normal relaxation.

Supplementary Information

A color picture of the new ESIPT fluorescent cellulose fibers, as well as the dyes in solid state, are shown in the Supplementary Information (Figure S1), and other data free of charge at <http://jbcs.sbq.org.br> as pdf file.

Acknowledgements

We are grateful for financial support and scholarships from the Brazilian agencies CNPq (Conselho Nacional de Desenvolvimento Científico e Tecnológico) and Fundação de Amparo à Pesquisa do Estado do Rio Grande do Sul (FAPERGS).

References

- Blotny, G.; *Tetrahedron* **2006**, *62*, 9507
- Blotny, G.; *Tetrahedron Lett.* **2003**, *44*, 1499.
- Zhang, P.; Yu, Y.-D.; Zhang, Z.-H.; *Synth. Commun.* **2008**, *38*, 4474.
- Haval, K. P.; *Synlett* **2006**, *13*, 2156.
- Giacomelli, G.; Porcheddu, A.; De Luca, L.; *Curr. Org. Chem.* **2004**, *8*, 1497.
- Duan, H. D.; Wang, L. Z.; Qin, D. W.; Li, X. M.; Wang, S. X.; Zhang, Y.; *Synth. Commun.* **2011**, *41*, 380.
- Mikhaylichenko, S. N.; Patel, S. M.; Dalili, S.; Chesnyuk, A. A.; Zaplishny, V. N.; *Tetrahedron Lett.* **2009**, *50*, 2505.
- Matloobi, M.; Schramm, H. W.; *J. Heterocycl. Chem.* **2010**, *47*, 724.
- Courme, C.; Gresh, N.; Lenoir, C.; Vidal, M.; Garbay, C.; Florent, J. C.; Bertounesque, E.; *Heterocycles* **2010**, *81*, 867.
- Bork, J. T.; Lee, J. W.; Khersonsky, S. M.; Moon, H. S.; Chang, Y. T.; *Org. Lett.* **2003**, *5*, 117.
- Moral, M.; Ruiz, A.; Moreno, A.; Diaz-Ortiz, A.; Lopez-Solera, I.; de la Hoz, A.; Sanchez-Migallon, A.; *Tetrahedron* **2010**, *66*, 121.
- Jan, J. Z.; Huang, B. H.; Lin, J.-J.; *Polymer* **2003**, *44*, 1003.
- Ren, S. J.; Zeng, D. L.; Zhong, H. L.; Wang, Y.; Qian, S.; Fang, Q.; *J. Phys. Chem. B* **2010**, *114*, 10374.
- Liu, B.; Qian, D. J.; Chen, M.; Wakayama, T.; Nakamura, C.; Miyake, J.; *Chem. Commun.* **2006**, *30*, 3175.
- Zhong, H. L.; Xu, E. J.; Zeng, D. L.; Du, J. P.; Sun, J.; Ren, S. J.; Jiang, B.; Fang, Q.; *Org. Lett.* **2008**, *10*, 709.
- Van Cott, K. E.; Amos, T.; Gibson, H. W.; Davis, R. M.; Heflin, J. R.; *Dyes Pigm.* **2003**, *58*, 145.
- Mahler, J.; Rafler, G.; *Opt. Mater.* **1999**, *12*, 363.
- Zhong, H. L.; Lai, H.; Fang, Q. A.; *J. Phys. Chem. C* **2011**, *115*, 2423.
- Omer, K. M.; Ku, S. Y.; Chen, Y. C.; Wong, K. T.; Bard, A. J.; *J. Am. Chem. Soc.* **2010**, *132*, 10944.
- Iijima, T.; Lee, C. H.; Fujiwara, Y.; Shimokawa, M.; Suzuki, H.; Yamane, K.; Yamamoto, T.; *Opt. Mater.* **2007**, *29*, 1782.
- Cai, Y.-Q.; Wu, W.; Wang, H.; Miyake, J.; Qian, D.-J.; *Surf. Sci.* **2011**, *605*, 321.
- Chen, H. F.; Yang, S. J.; Tsai, Z. H.; W. Y. Hung, Wang, T. C.; Wong, K. T.; *J. Mater. Chem.* **2009**, *19*, 8112.
- Rothmann, M. M.; Haneder, S.; Da Como, E.; Lennartz, C.; Schildknecht, C.; Strohriegel, P.; *Chem. Mater.* **2010**, *22*, 2403.
- De Hoog, P.; Gamez, P.; Driessen, W. L.; Reedijk, J.; *Tetrahedron Lett.* **2002**, *43*, 6783.
- Gorenssek, M.; *Dyes Pigm.* **1999**, *40*, 225.
- Taylor, J. A.; Pasha, K.; Phillips, D. A. S.; *Dyes Pigm.* **2001**, *51*, 145.

27. Um, S. I.; Lee, J. K.; Kang, Y.; Baek, D. J.; *Dyes Pigm.* **2006**, *70*, 84.
28. Son, Y. A.; Hong, J. P.; Lim, H. T.; Kim, T. K.; *Dyes Pigm.* **2005**, *66*, 231.
29. Czajkowski, W.; Paluszkiwicz, J.; Stolarski, R.; Kaźmierska, M.; Grzesiak, E.; *Dyes Pigm.* **2006**, *71*, 224.
30. Seo, J.; Kim, S.; Park, S. Y.; *J. Am. Chem. Soc.* **2004**, *126*, 11154.
31. Jung, H. S.; Kim, H. J.; Vicens, J.; Kim, J. S.; *Tetrahedron Lett.* **2009**, *50*, 983.
32. Yang, C.-C.; Tian, Y.; Chen, C.-Y.; Jen, A. K.-Y.; Chen, W.-C.; *Macromol. Rapid Commun.* **2007**, *28*, 894.
33. Wu, Y. K.; Peng, X. J.; Fan, J. L.; Gao, S.; Tian, M. Z.; Zhao, J. Z.; Sun, S.; *J. Org. Chem.* **2007**, *72*, 62.
34. Klymchenko, A. S.; Demchenko, A. P.; *J. Am. Chem. Soc.* **2002**, *124*, 12372.
35. Rodembusch, F. S.; Campo, L. F.; Rigacci, A.; Stefani, V.; *J. Mater. Chem.* **2005**, *15*, 1537.
36. Kober, U. A.; Campo, L. F.; Costa, T. M. H.; Stefani, V.; Gallas, M. R.; *J. Photochem. Photobiol., A* **2007**, *186*, 24.
37. Rodembusch, F. S.; Leusin, F. P.; Bordignon, L. B.; Gallas, M. R.; Stefani, V.; *J. Photochem. Photobiol., A* **2005**, *153*, 81.
38. Joule, J. A.; Mills, K.; *Heterocyclic Chemistry*, 4th ed.; Blackwell Science: Cambridge, 2000.
39. Campo, L. F.; Corrêa, D. S.; Araújo, M. A.; Stefani, V.; *Macromol. Rapid Commun.* **2000**, *21*, 832.
40. Douhal, A.; Amat-Guerri, F.; Lillo, M. P.; Acuña, A. U.; *J. Photochem. Photobiol., A* **1994**, *78*, 127.
41. Nagaoka, S. I.; Kusunoki, J.; Fujibuchi, T.; Hatakenaka, S.; Mukai, K.; Nagashima, U.; *J. Photochem. Photobiol., A* **1999**, *122*, 151.
42. Guallar, V.; Moreno, M.; Lluch, J. M.; Amat-Guerri, F.; Douhal, A.; *J. Phys. Chem.* **1996**, *100*, 19789.
43. Santra, S.; Dogra, S. K.; *Chem. Phys.* **1998**, *226*, 285.
44. Rodembusch, F. S.; Campo, L. F.; Leusin, F. P.; Stefani, V.; *J. Lumin.* **2007**, *126*, 728.

Submitted: August 1, 2011

Published online: October 11, 2011

Supplementary Information

Synthesis, Characterization and Photophysical Properties of ESIPT Reactive Triazine Derivatives

Marcelo D. Kuplich, Fábio S. Grasel, Leandra F. Campo,
Fabiano S. Rodembusch and Valter Stefani*

Laboratório de Novos Materiais Orgânicos, Instituto de Química, Universidade Federal do
Rio Grande do Sul, Av. Bento Gonçalves 9500, CP 15003, 91501-970 Porto Alegre-RS, Brazil

Picture of the dyes and stained cellulose under normal light
and UV radiation

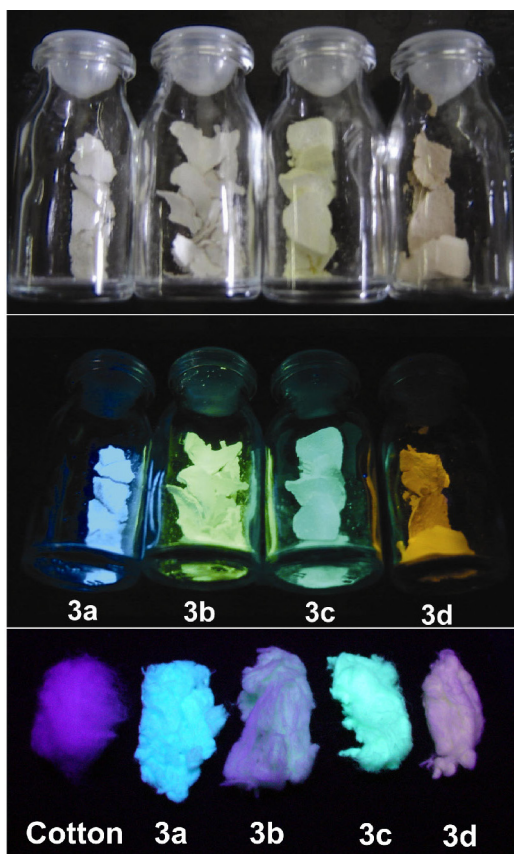


Figure S1. Triazine derivatives under normal light (top) and UV light (middle) and the respective ESIPT fluorescent cellulosic fibers under UV light (bottom).

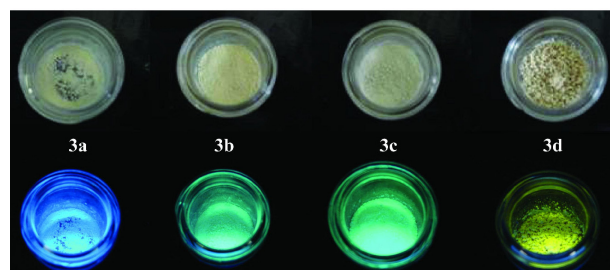


Figure S2. Triazine derivatives under normal light (top) and UV light (bottom).

Original spectroscopic data

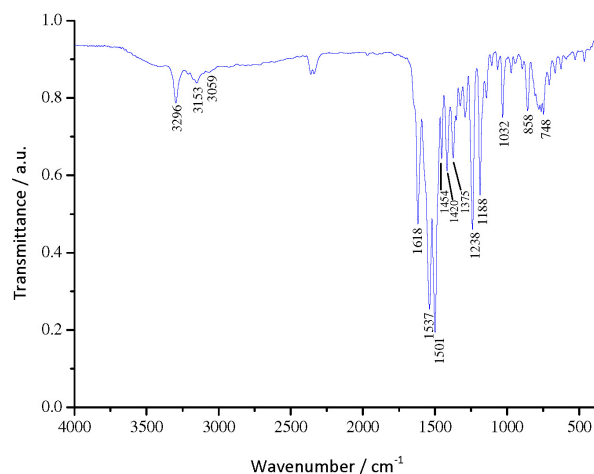


Figure S3. FTIR spectrum of the dye 3a in KBr pellets.

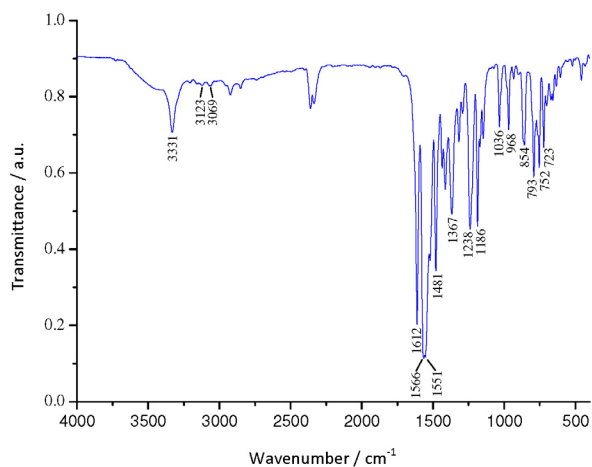


Figure S4. FTIR spectrum of the dye **3b** in KBr pellets.

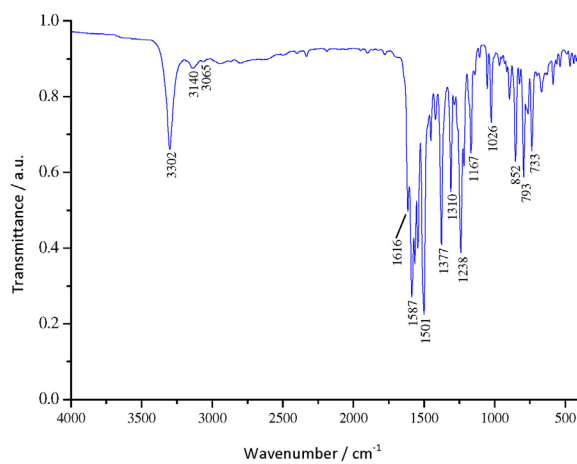


Figure S5. FTIR spectrum of the dye **3c** in KBr pellets.

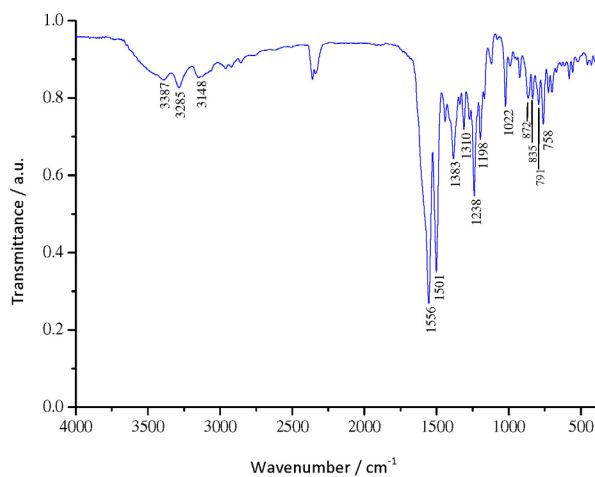


Figure S6. FTIR spectrum of the dye **3d** in KBr pellets.

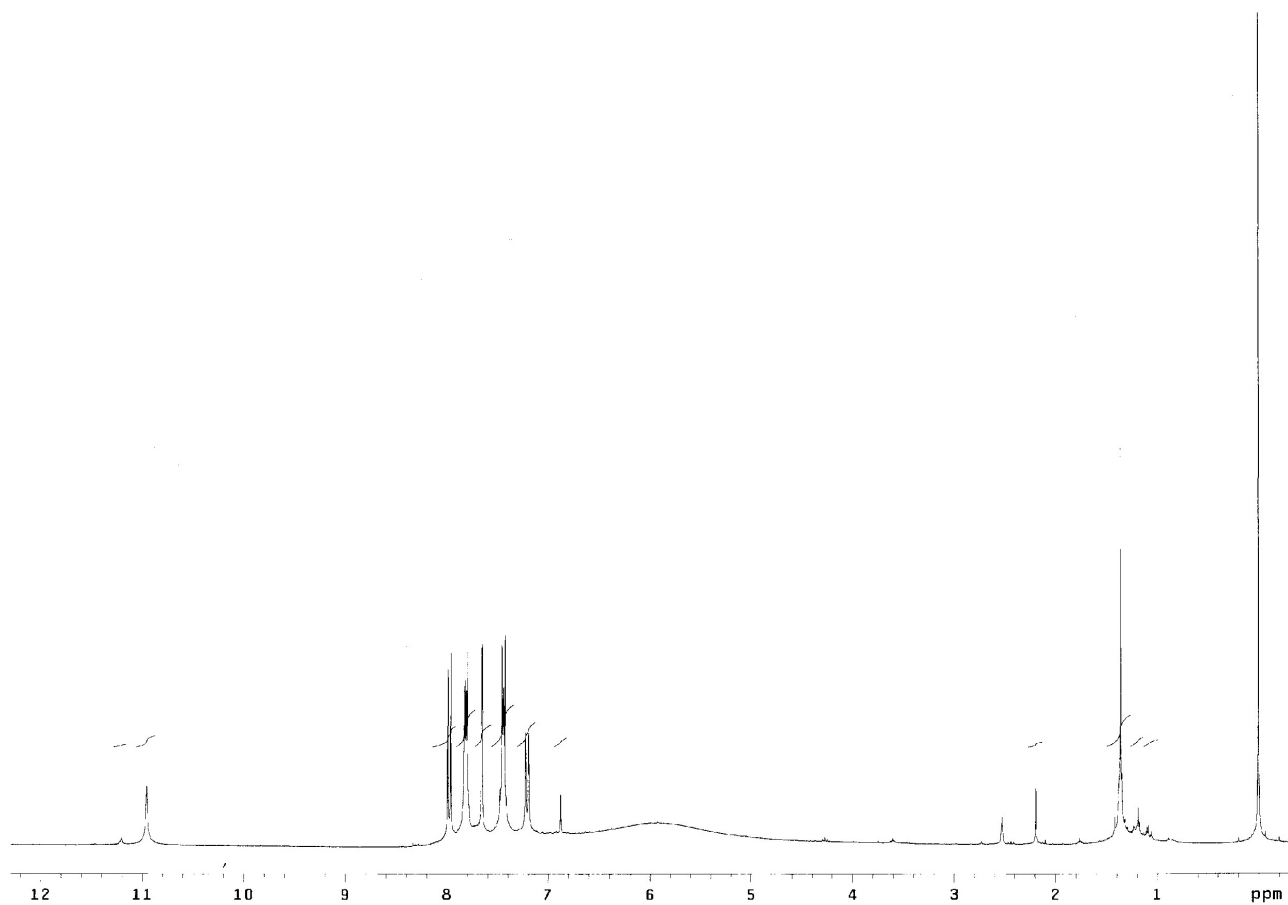


Figure S7. ^1H NMR spectrum of the dye **3a** (300 MHz, $\text{DMSO-}d_6$).

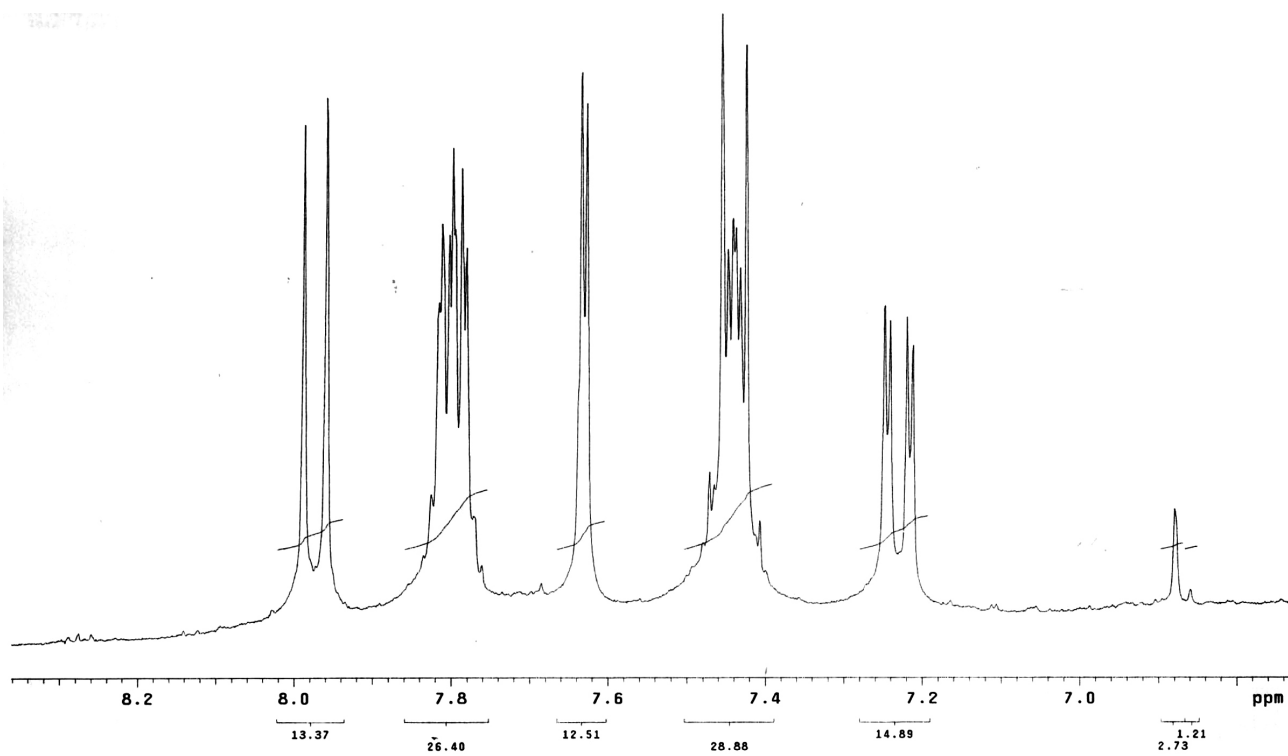


Figure S8. ^1H NMR spectrum of the dye **3a** (zoom of the aromatic region).

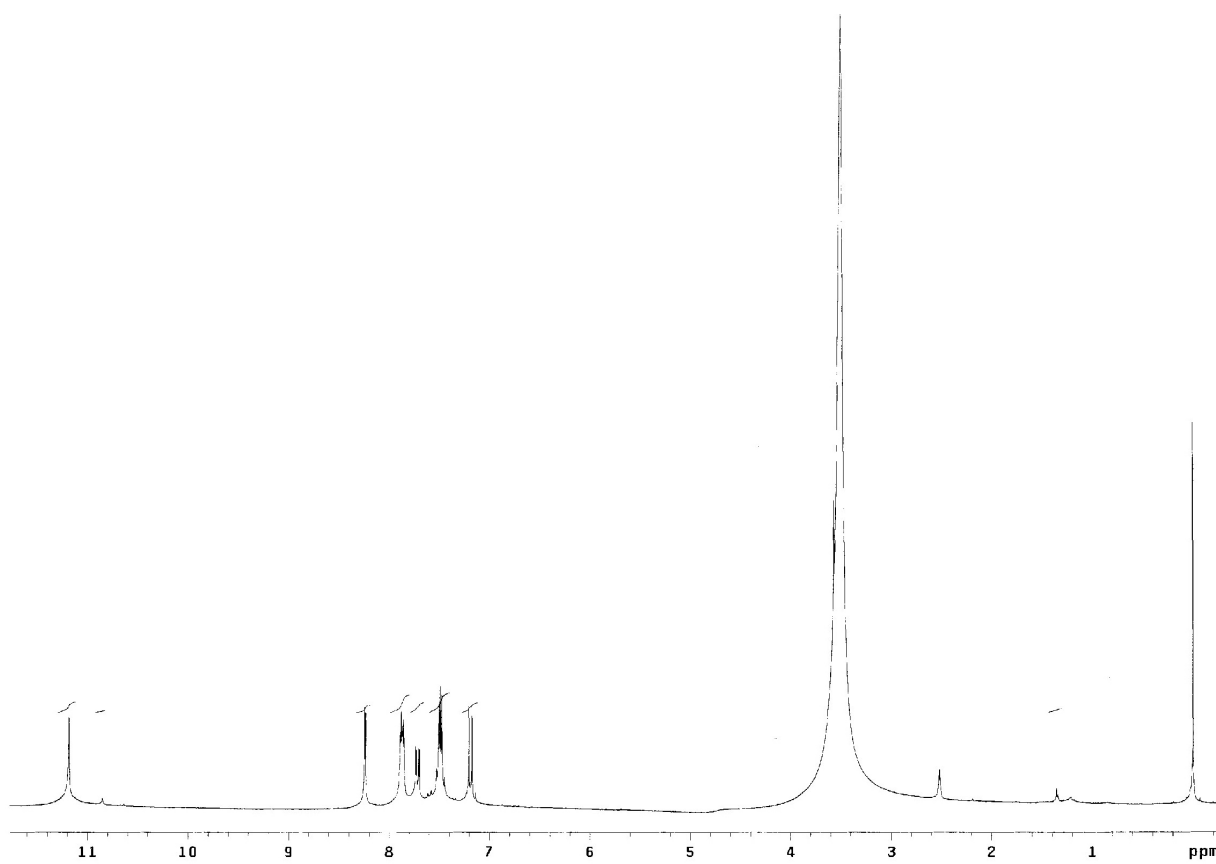


Figure S9. ^1H NMR spectrum of the dye **3b** (300 MHz, $\text{DMSO-}d_6$).

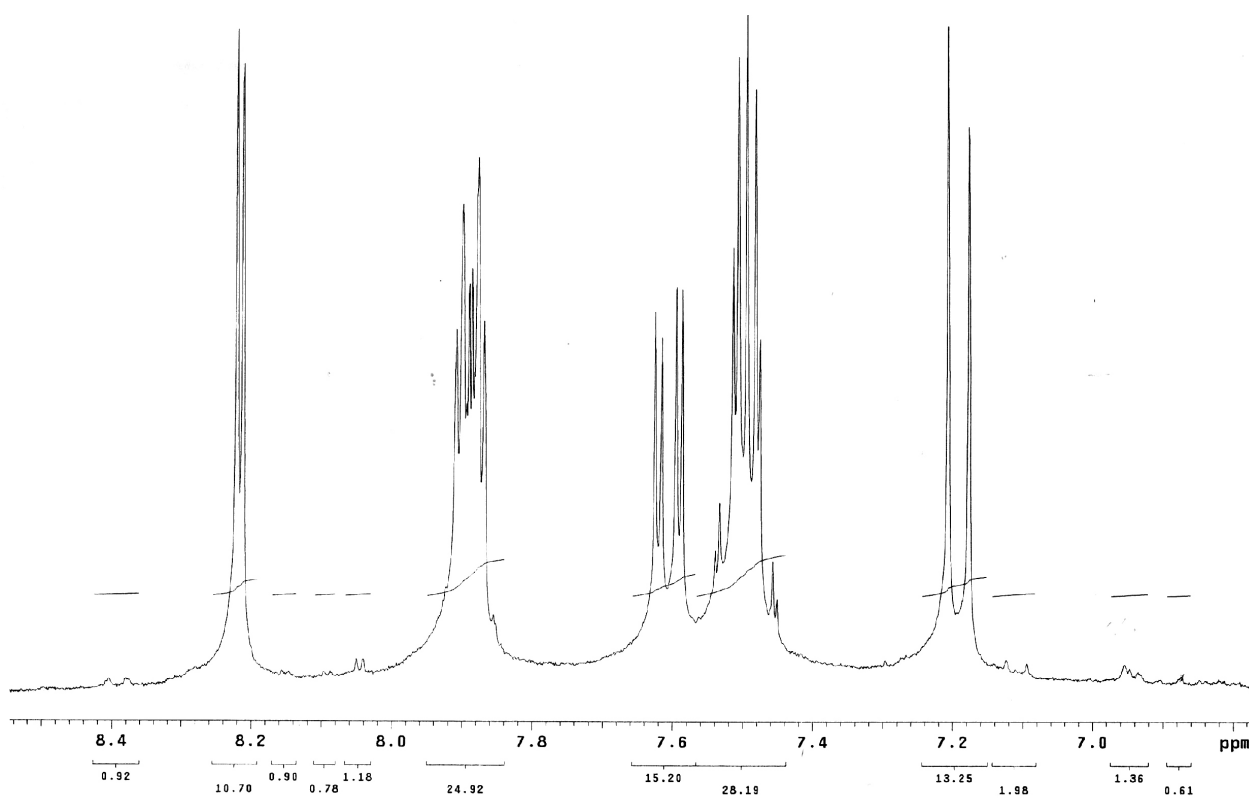


Figure S10. ^1H NMR spectrum of the dye **3b** (zoom of the aromatic region).

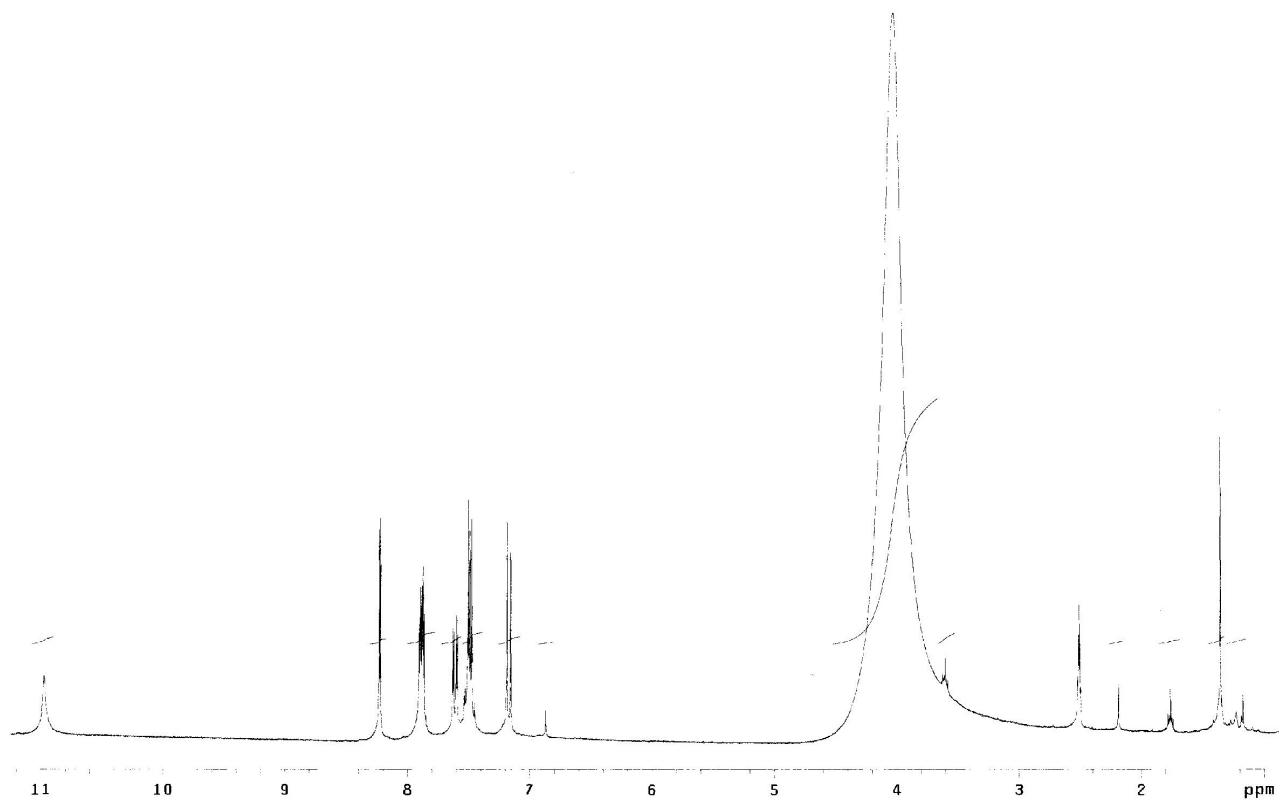


Figure S11. ^1H NMR spectrum of the dye **3c** (300 MHz, $\text{DMSO}-d_6$).

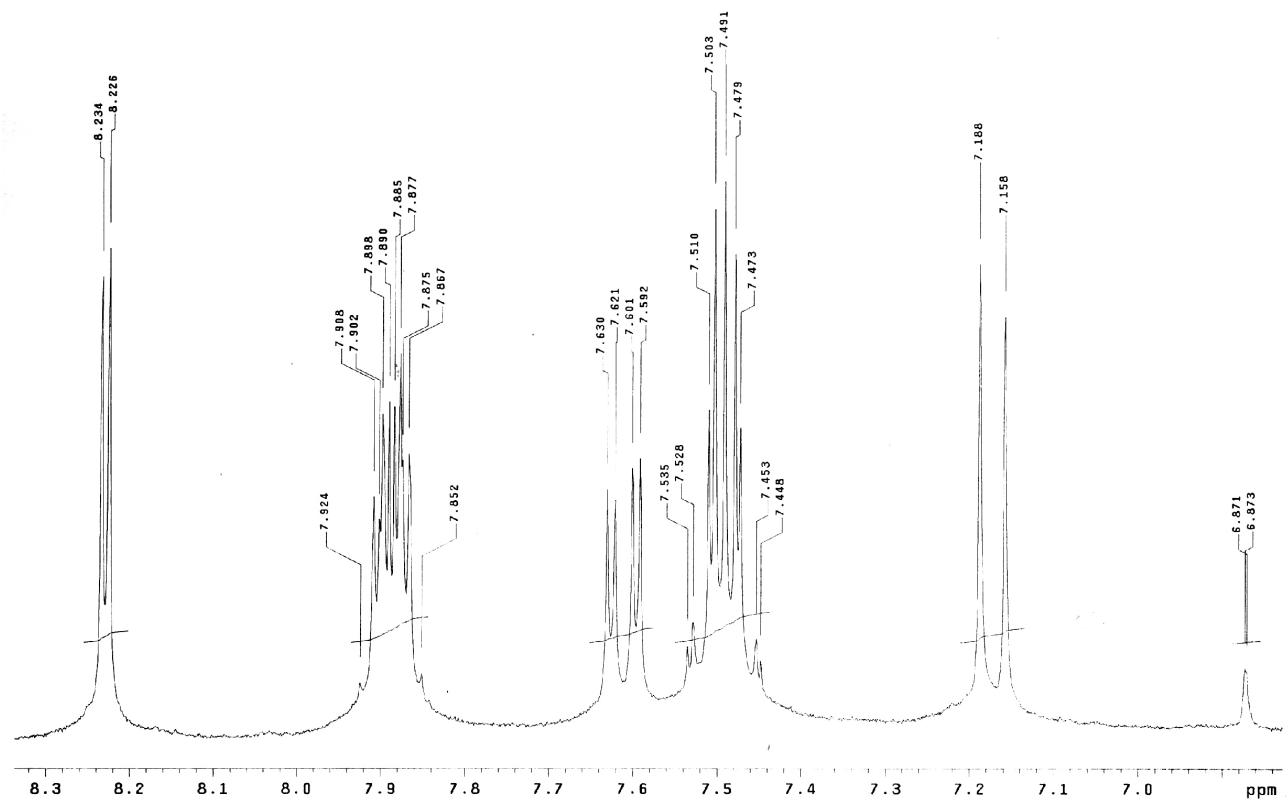


Figure S12. ^1H NMR spectrum of the dye **3c** (zoom of the aromatic region).

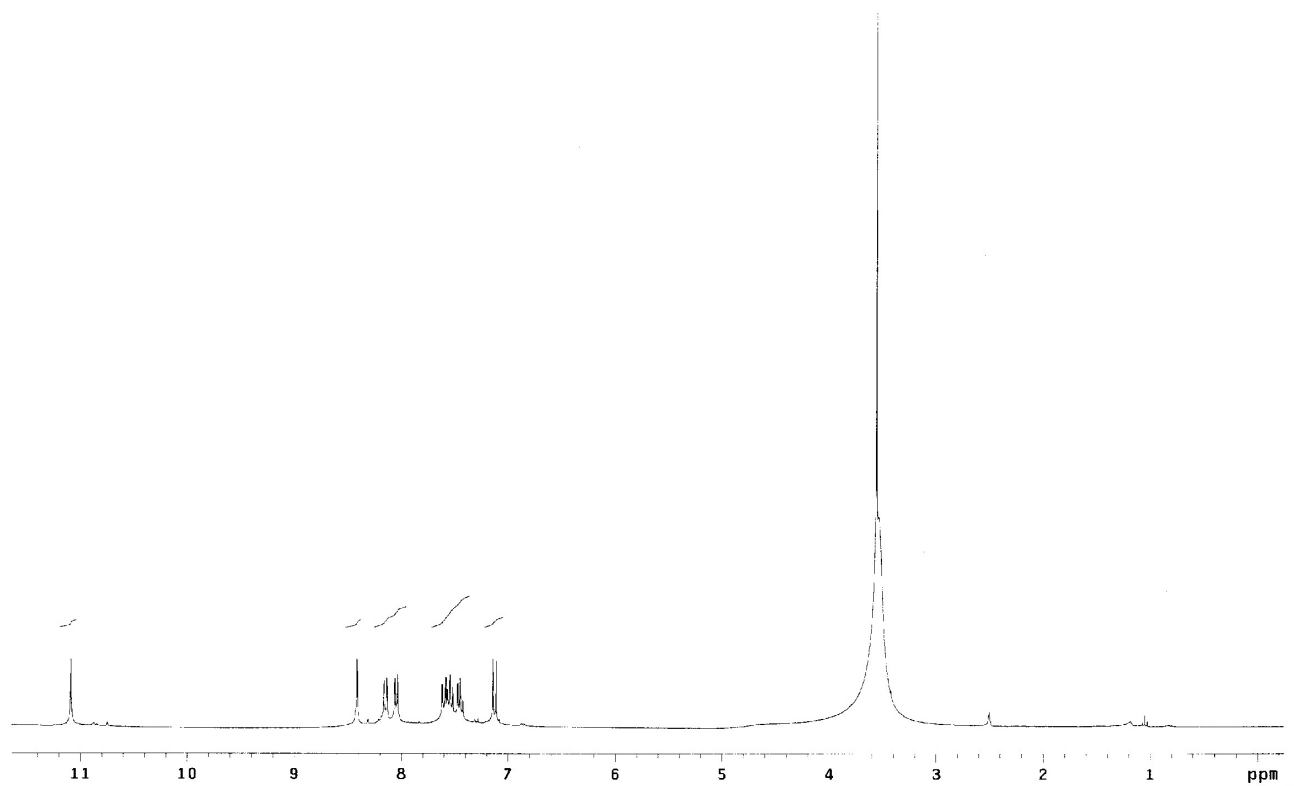


Figure S13. ¹H NMR spectrum of the dye **3d** (300 MHz, DMSO-*d*₆).

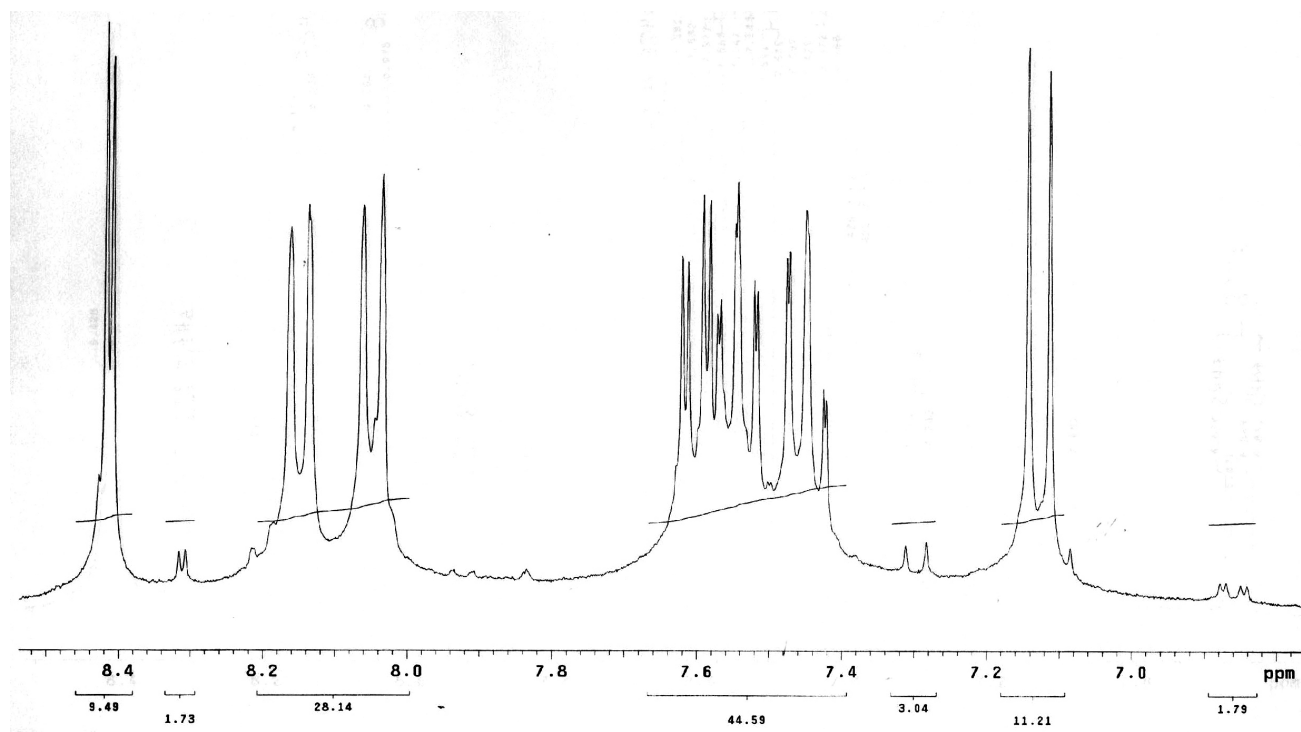


Figure S14. ¹H NMR spectrum of the dye **3d** (zoom of the aromatic region).

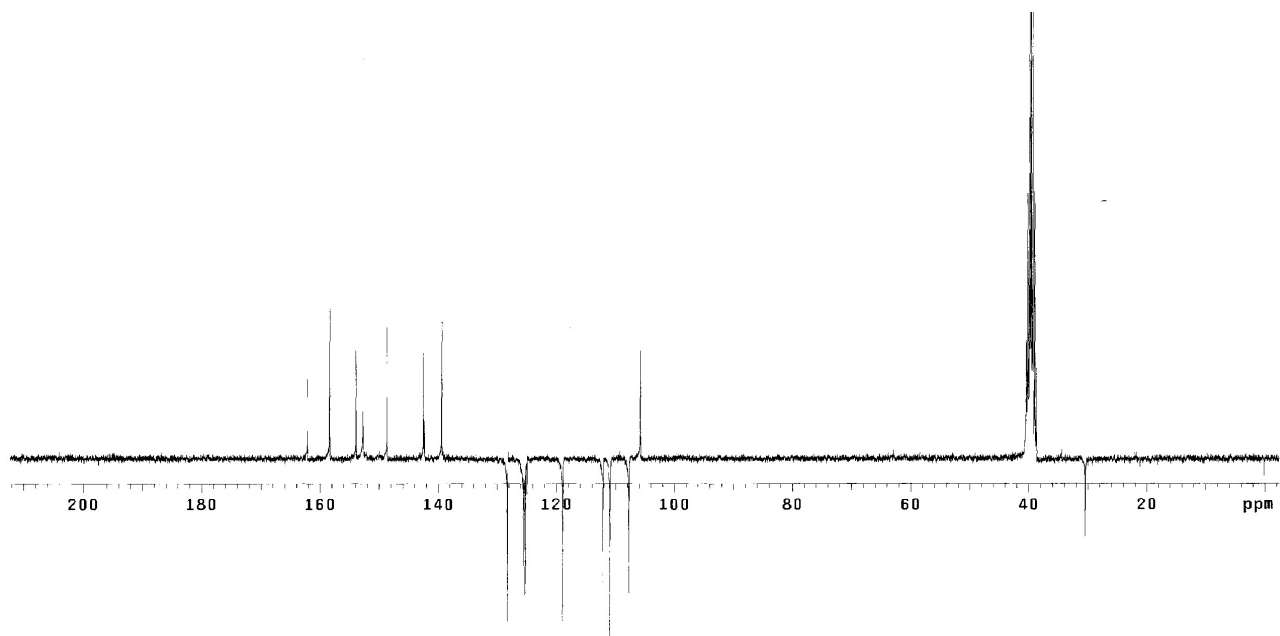


Figure S15. ^{13}C NMR (APT) spectrum of the dye **3a** (75 MHz, $\text{DMSO}-d_6$).

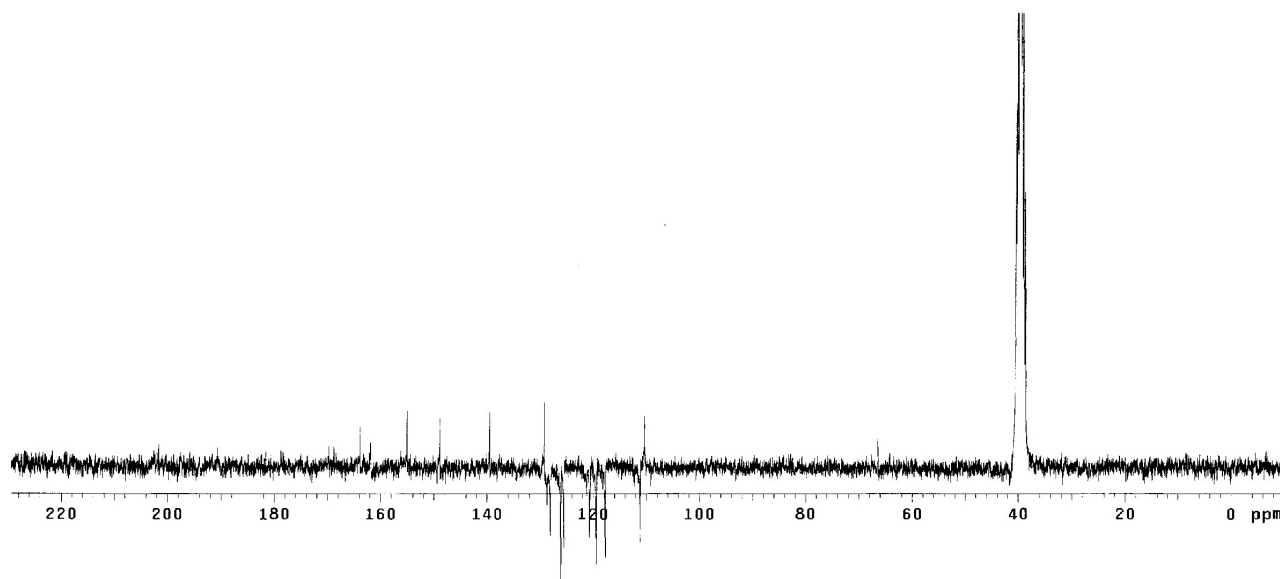


Figure S16. ^{13}C NMR (APT) spectrum of the dye **3b** (75 MHz, $\text{DMSO}-d_6$).

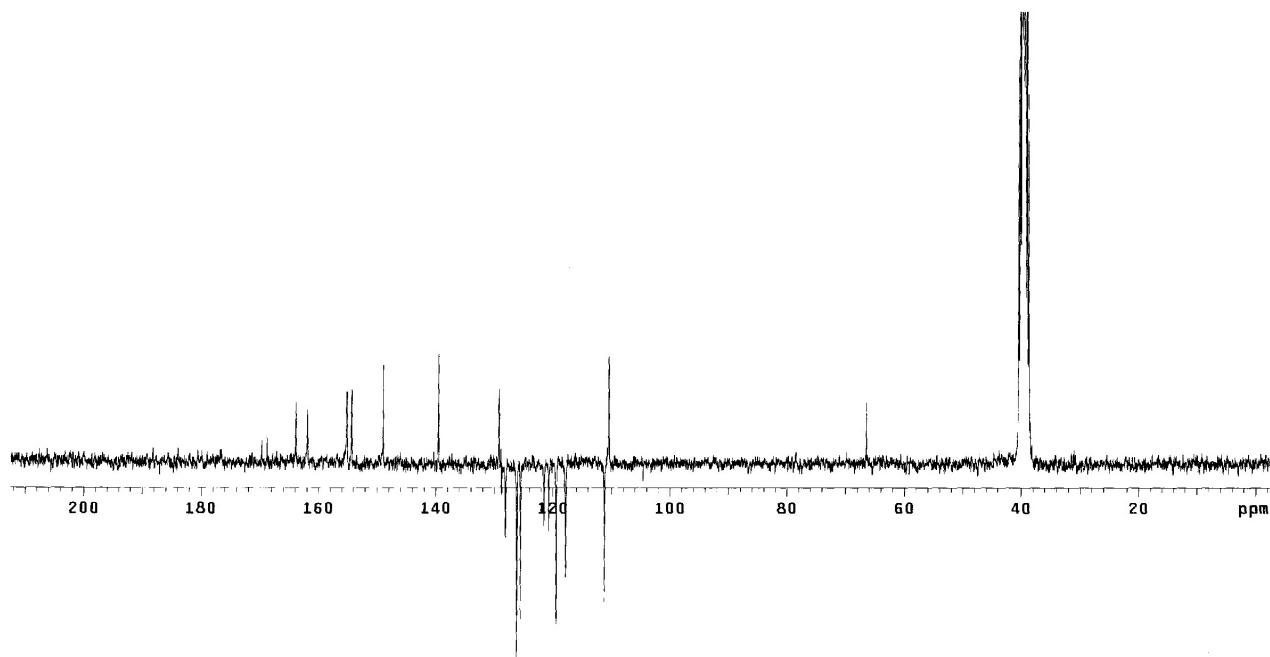


Figure S17. ¹³C NMR (APT) spectrum of the dye **3c** (75 MHz, DMSO-*d*₆).

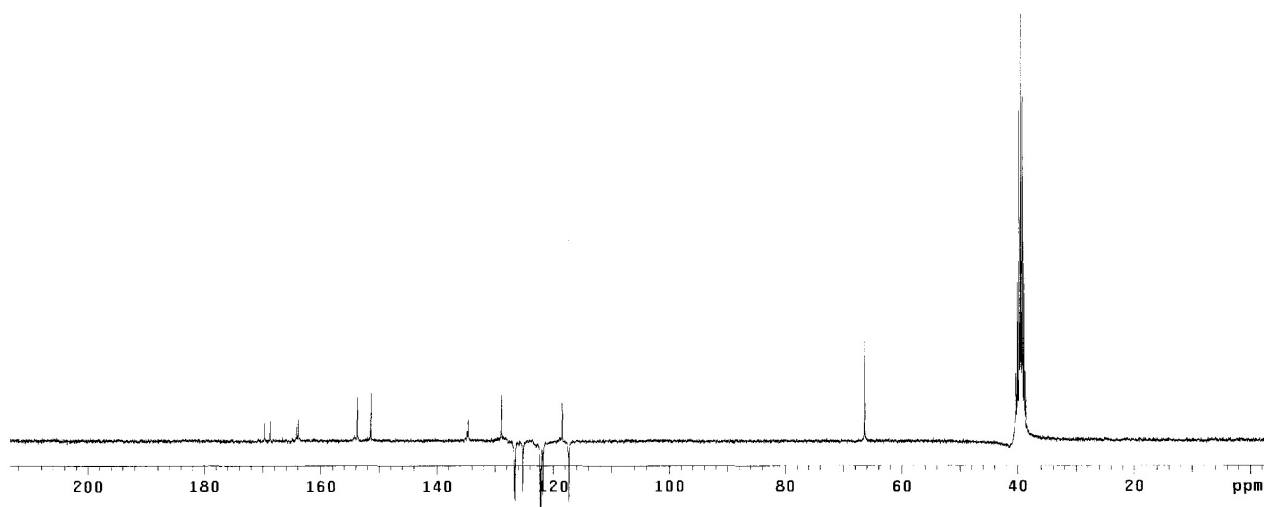


Figure S18. ¹³C NMR (APT) spectrum of the dye **3d** (75 MHz, DMSO-*d*₆).